American Heart Association | American Stroke Association

Imaging Cardiovascular Calcification

Ying Wang, MD, PhD; Michael T. Osborne, MD; Brian Tung, MS; Ming Li, MD, PhD; Yaming Li, MD, PhD

Cardiovascular disease is the leading cause of morbidity and mortality worldwide. Atherosclerosis is a complex and multifactorial process, characterized by early asymptomatic formation of plaque in the arterial walls, silent plaque progression that poses flow limitation, and risk of sudden rupture and subsequent thrombotic occlusion.[1] The early assessment and predictive value of atherosclerotic plaque development and rupture are critically important to prevent clinical consequences.

Inflammation and calcification play important roles in the pathophysiological progression of atherosclerosis. In the early stage, inflammation is the predominant process involved that promotes plaque progression and calcification.[2] The repeated cycles of inflammatory damage and repair ultimately lead to calcification of the vessel walls,[3] whose extent provides an important estimate of atherosclerotic progression and clinical prognosis. Macrocalcification is considered the stable stage of vascular disease, whereas the dynamic process of microcalcification may increase the risk of plaque rupture and adverse clinical events.[4] Therefore, imaging early calcification is important to identify individuals with enhanced risk of cardiovascular events. Furthermore, many studies have demonstrated coronary artery calcification as a marker for the extent of atherosclerosis and overall plaque burden, and as an important independent predictor of cardiovascular events, mortality, and morbidity.[5–8] Over the past few decades, advanced imaging methods have improved our assessment of atherosclerotic calcification and have provided insights into cardiovascular risk and have contributed to the understanding of the underlying pathophysiologic mechanisms of atherosclerosis.

This review aims to summarize current imaging techniques for vascular calcification (Table) and their applications in clinical research.

Atherosclerosis Development, Calcification, and Progression

Atherosclerosis exists as a pathological continuum. The persistence of vascular risk factors promotes dysfunction of vascular endothelium and increases its permeability, allowing apolipoproteins to enter the intima and become oxidized. The formation of oxidized apolipoprotein and the expression of cellular adhesion molecules, monocyte chemotactic protein 1, and other chemokines from the endothelium induce monocytes to migrate into the intima and differentiate into macrophages. These macrophages secrete additional inflammatory cytokines and extracellular matrix molecules, while engulfing oxidized lipoproteins to form lipid-laden foam cells. When the amount of oxidized lipoproteins engulfed by macrophages exceeds their clearance capacities, the foam cells undergo apoptosis and release lipoproteins and other cellular contents, which lead to the formation of an extracellular lipid core and contribute to lipid-rich plaque accumulation within the arterial wall.[9] Over time, these atheromatous plaques undergo a series of processes (eg, hypoxia, neovascularization, and microcalcification).

Vascular calcification is a complex, organized, regulated, and active progress, much like the formation of bone. In fact, macrophages in atherosclerotic plaques promote osteogenic differentiation by releasing pro-inflammatory cytokines (eg, IL-1, IL-6, IL-8, and tumor necrosis factor-α). The resulting microcalcification crystals initiate a positive feedback loop by further stimulating the pro-inflammatory response of macrophages, thereby propagating the pro-calcific stimulus in the vascular wall.[10]

Vascular calcification can be classified into 2 distinct forms, depending on its location within the intima (intimal calcification) or in the vascular medial (medial calcification) layer. Calcification of the arterial vessel's intimal and medial

From the Department of Nuclear Medicine, First Hospital of China Medical University, Shenyang, Liaoning, China (Y.W., Y.L.); Department of Radiology (Y.W., M.T.O., B.T.) and Cardiology Division (M.T.O.), Massachusetts General Hospital, Boston, MA; Department of Urology, Shengjing Hospital of China Medical University, Shenyang, Liaoning, China (M.L.).

Correspondence to: Yaming Li, MD, PhD, FACNM, Department of Nuclear Medicine, First Hospital of China Medical University, No. 155 North Nanjing St, Heping District, Shenyang City, Liaoning Province 110001, China. E-mail: ymli2001@163.com

J Am Heart Assoc. 2018;7:e008564. DOI: 10.1161/JAHA.118.008564.

Table. Current Imaging Techniques for Vascular Calcification

Approach	Advantages	Disadvantages	Macrocalcification	Microcalcification	Invasive
IVUS	Directly image the vessel wall. Ability to detect hyperechoic calcified plaque	Limited axial resolution. Limited ability in accurate assessment of plaque composition. Inability to detect microcalcification	✓		✓
CACS	Provide a simple, rapid and reliable quantification of macroscopic calcium, and the total coronary calcification burden	Lower resolution and poor tissue contrast. Inability to provide information on plaque morphology or subtype	✓		
CCTA	High spatial and temporal resolution. Ability to estimate the severity of coronary stenosis and provide detailed information on plaque morphology	Requires the administration of contrast agent. Difficulty in identifying and quantifying calcium in the presence of iodine in contrast media	✓		
MRI	Superior soft-tissue resolution. Lack of ionizing radiation. Multipulse sequences can depict the location and volume of vascular calcification	Prolonged acquisition time. Motion artifacts during the cardiac contractions and respiration. Inability to identify microcalcification	✓		
OCT	High spatial resolution. Capable of assessing fibrous cap thickness, macrophage filtration, the thickness and border of vascular calcification	Difficult to differentiate calcium and lipid pool. Limited tissue penetration	✓		✓
Invasive angiography	Superior spatial resolution and temporal resolution. The criterion standard for coronary atherosclerosis imaging	Inability to provide direct imaging of calcification or the atherosclerotic plaque itself			✓
^{18}F-NaF PET	Exquisite sensitivity. Capable of identifying microcalcification and the vulnerable plaque	Relatively lower spatial resolution. Continuous cardiac motion prevents accurate quantification of coronary artery microcalcification		✓	
^{18}F-FDG PET/CT	Attenuated-CT can visualize the bulky macrocalcification	Background myocardial uptake limited its assessment of coronary arteries	✓		

CACS indicates coronary artery calcium score; CCTA, coronary computed tomographic angiography; CT, computed tomography; FDG, 2-deoxy-2-fluoro-D-glucose; IVUS, intravascular ultrasound; MRI, magnetic resonance imaging; OCT, optical coherence tomography; PET, positron emission tomography.

layer is presumed to have a different pathogenesis and clinical consequences.[11] The intimal layer consists of endothelial cells that undergo a series of processes and eventually form atheromatous plaques that can cause plaque rupture and subsequent thromboembolic events,[12] whereas the medial layer consists of smooth muscle cells and elastic fibers that can regulate blood flow and arterial pressure. Calcification of the media is thought to cause arterial stiffening, reduce compliance, and limit distensibility. Presently, ex vivo histological analysis is the criterion standard to distinguish intimal and medial calcification.[11]

Vascular calcification occurs in a 2-phase process: an initial stage of microcalcification and the subsequent stage of macroscopic calcium formation (macrocalcification).[13] Although there is no conventional standard of size, there is general consensus that categorizes microcalcification and macrocalcification based on nodules of <50 and ≥ 50 μm, respectively.[14]

Microcalcification, a clinically more significant manifestation of vascular mineralization, represents the early stages of intimal calcium formation and greatly amplifies mechanical stresses on the surface of the fibrous plaque that may directly contribute to its rupture.[4,14] Detection of microcalcification is not possible with current clinical computed tomography (CT) systems, which are only able to identify large areas of macrocalcification of 200 to 500 μm in diameter.[15] However, these structures can now be detected noninvasively using molecular imaging. Indeed, because of preferential adsorption of fluoride to areas of microcalcification, ^{18}F-NaF is the only currently available clinical imaging platform that can noninvasively detect

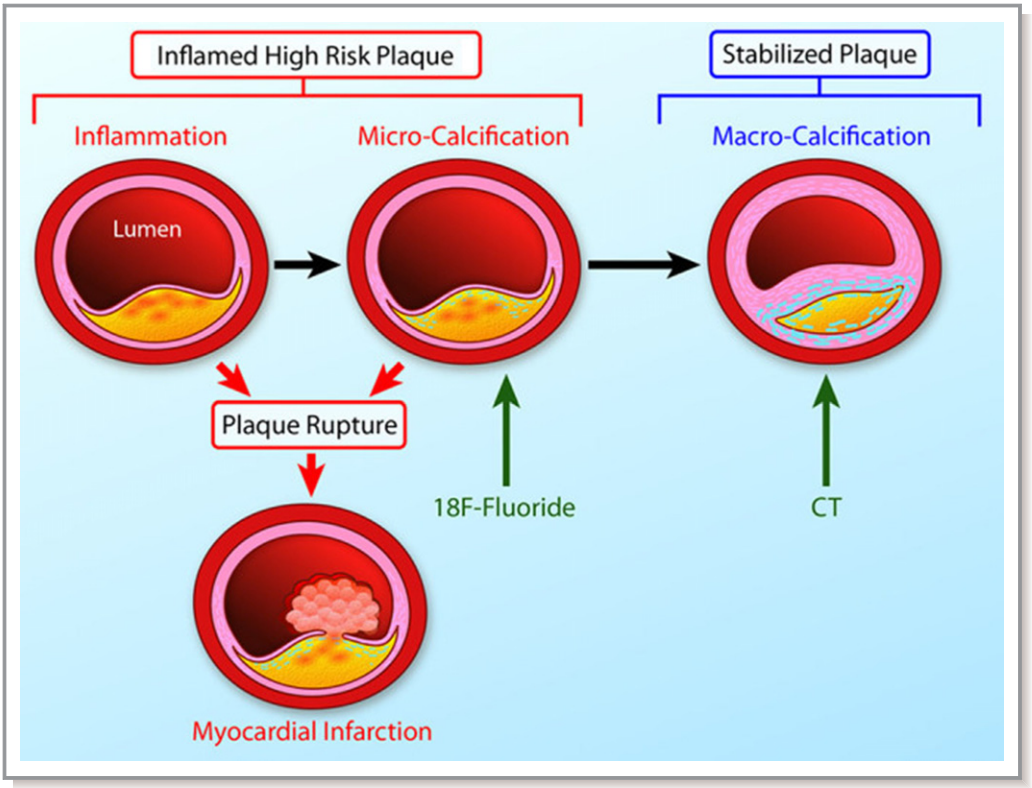

Figure 1. The link between inflammation, microcalcification, and macrocalcification. A large necrotic core, a thin fibrous cap, and an intense inflammation are key precipitants of acute plaque rupture and myocardial infarction. Intimal calcification is thought to occur as a healing response to this intense necrotic inflammation. However, the early stages of microcalcification (detected by ^{18}F-fluoride positron emission tomography) are conversely associated with an increased risk of rupture. In part, this is because of residual plaque inflammation and in part because microcalcification itself increases mechanical stress in the fibrous cap, further increasing propensity to rupture. With progressive calcification, plaque inflammation becomes pacified and the necrotic core is walled off from the blood pool. The later stages of macrocalcification (detected by noninvasive imaging techniques such as computed tomography [CT] and magnetic resonance imaging [MRI], and by invasive imaging techniques such as intravascular ultrasound and optical coherence tomography) are, therefore, associated with plaque stability and a lower risk of that plaque rupturing (Illustration credit: Ben Smith). Reprinted from Dweck et al[16] with permission. Copyright ©2016, Wolters Kluwer Health, Inc. Promotional and commercial use of the material in print, digital or mobile device format is prohibited without the permission from the publisher Wolters Kluwer. Please contact permissions@lww.com for further information.

microcalcification in active unstable atheroma. The preferential binding of ^{18}F-NaF to microcalcification is because of the high surface area of hydroxyapatite in these nanocrystalline areas.[16] Irkle et al[17] used autoradiography, whereby dispersion in large tissues and the lack of physical barriers increased adsorption of ^{18}F-NaF to microcalcifications.

With progressive calcification, plaque inflammation becomes pacified with its necrotic core walled off from the blood pool. The latter stages of macrocalcification are, therefore, associated with plaque stability and lower risk of plaque rupture. Macrocalcifications have a large volume but small surface area; much of the hydroxyapatite is internalized and not available for binding with ^{18}F-fluoride.[16] Moreover, ^{18}F-NaF cannot penetrate into its deeper layers.[14,17] ^{18}F-NaF only bound to the outer surface of the macrocalcifications. Thus, ^{18}F-NaF cannot characterize macrocalcification exactly. However, morphologic calcific imaging techniques such as CT, ultrasound, and magnetic resonance imaging (MRI) are readily available to identify the macrocalcification because of their superb spatial resolution.

An illustration of this pathophysiologic progression and current imaging techniques for vascular calcification are portrayed in Figures 1 and 2.[16,18–23]

Multimodality Imaging Techniques

Computed Tomography

CT is the most established noninvasive tool to detect coronary artery calcium (CAC). It can provide a simple, rapid, and

reliable quantification of macroscopic calcium[24] and generate a clinical CAC score (CACS). In the 1990s, quantification of CAC on non-contrast-enhanced ECG gated CT examination became recognized as an important noninvasive imaging technique for identifying coronary atherosclerosis.[25]

CACS relies upon the high attenuation coefficient of calcium to detect calcified plaques.[26] The standard method of scoring is the Agatston method.[25] The Agatston score considers total calcified area and maximum density of calcification (>130 Hounsfield units [HU]) to provide a summed score of all calcified lesions. Although other methods of scoring have been used, the Agatston score remains the criterion standard because of its simplicity.

CACS provides quantification of the total coronary calcification burden and has become a useful clinical tool for risk stratification in asymptomatic patients with low-to-intermediate and intermediate risk of cardiovascular events.[27,28] It predicts future cardiovascular risk beyond the traditional Framingham risk score alone.[29–32] An elevated CACS may portend an increased risk of cardiovascular events in some patients.[33] Specifically, the MESA study (Multi-Ethnic Study of Atherosclerosis) with 6722 patients followed for an average of 3.8 years showed that those with CACS >300 have a nearly 10-fold increased risk of coronary event across ethnic groups.[34] Shah et al[35] investigated the prognostic significance of calcified plaque among symptomatic patients with nonobstructive coronary artery disease. Their results also showed that among patients with detectable mild luminal stenosis, 4-year mortality rates ranged from 0.8% to 9.8% for CAC scores of 0 to ≥400, but among patients with no luminal stenosis, CAC was not predictive of all-cause mortality. Moreover, Mori et al[36] demonstrated that CAC associates with cardiovascular events in a stepwise fashion, providing meaningful risk stratification for future coronary events with the additional knowledge that a low CACS is associated with low risk for cardiovascular mortality, which was also supported by the study of Sarwar et al[37]

However, Puri et al[38] observed that dense calcium deposition on CT imaging seems to indicate plaque stability, and it progresses with age. As such, Nakahara et al[39] regard that dense calcification (>400 HU) is usually associated with stable plaques, although coronary calcification is a marker of coronary atheroma. Thus, a high CACS is perhaps more useful as a marker of vascular disease burden than as a predictor of the likelihood of a cardiovascular event from an individual plaque, which was reinforced by studies[40,41] showing that patients with stable disease were more heavily calcified than those with unstable disease. Furthermore, a recent investigation of 4425 patients evaluated composition of the plaque and showed that 1021 had only calcified plaques,183 had only noncalcified plaques, and 685 had both calcified and noncalcified plaques. Among these groups, the incidences of cardiovascular disease (CVD) events over a median follow-up of 3 years were 5.5%, 22.7%, and 37.7%, respectively.[8]

Furthermore, statin is the treatment choice to lower total cholesterol and low-density lipoprotein and has been extremely successful in primary and secondary prevention of CVD.[42] In spite of achieving the target reduction in low-density lipoprotein, many clinical trials[43–47] and a meta-analysis[48] have shown that statin therapy increased the progression of CAC compared with placebo in the absence of a higher event rate.[43] In both primate[49] and swine[50] models, anti-atherosclerotic interventions are associated with an increase in vascular fibrous tissue and calcification. Calcium deposition continues during the initial phase of plaque regression because of the death of foam cells and an increase in necrotic tissue. Thus, vascular calcification may have a key role in the initial stabilization of atherosclerotic plaques. Many researchers[51–54] now agree that statins likely have their salutary effects on CVD risk by reducing the lipid core in unstable plaques and activating plaque repair and healing by increasing the replacement of the lipid core with fibrosis and calcification. Eventually this process increases calcium density in such plaques and yields a reduction in CVD events through plaque stabilization.

Several hypotheses have arisen in an effort to explain these seemingly divergent findings. Specifically, Pugliese et al[55] hypothesized that the discrepancy between CACS and cardiovascular risk might be related to the fact that CT imaging does not have the ability to differentiate between quiescent and active calcification. Cowell et al[56] hypothesized that the morphologic imaging of CT better characterizes the structural aspects of calcification in atherosclerotic plaques than the pathological process of calcification. Other studies of culprit plaques[4,57] have also concluded that CT imaging is only able to identify macrocalcification and not the higher-risk microcalcification that occurs at earlier stages of disease.

Additional work has refined the clinical implications of CAC imaging findings. Criqui et al[58] reported that the use of the Agatston score in assessing CAC progression is problematic since an increase in CAC could be caused by an increase in volume, an increase in density, or both. So despite the studies suggesting a strong predictive value of CAC for CVD, there has been little rigorous comparison of what specific measure of CAC is most predictive.[59] In order to clarify the clinical significance of these factors, Criqui et al[58] conducted a multicenter, prospective observational study of the MESA cohort to determine the independent associations of CAC volume and CAC density with incident CVD events. Their results demonstrated that CAC density was inversely related to CVD events for a given CAC volume and that CAC volume was more predictive and was positively and independently associated with coronary artery disease and CVD risk when adjusted for CAC density. Thus, CAC may not be a monolithic

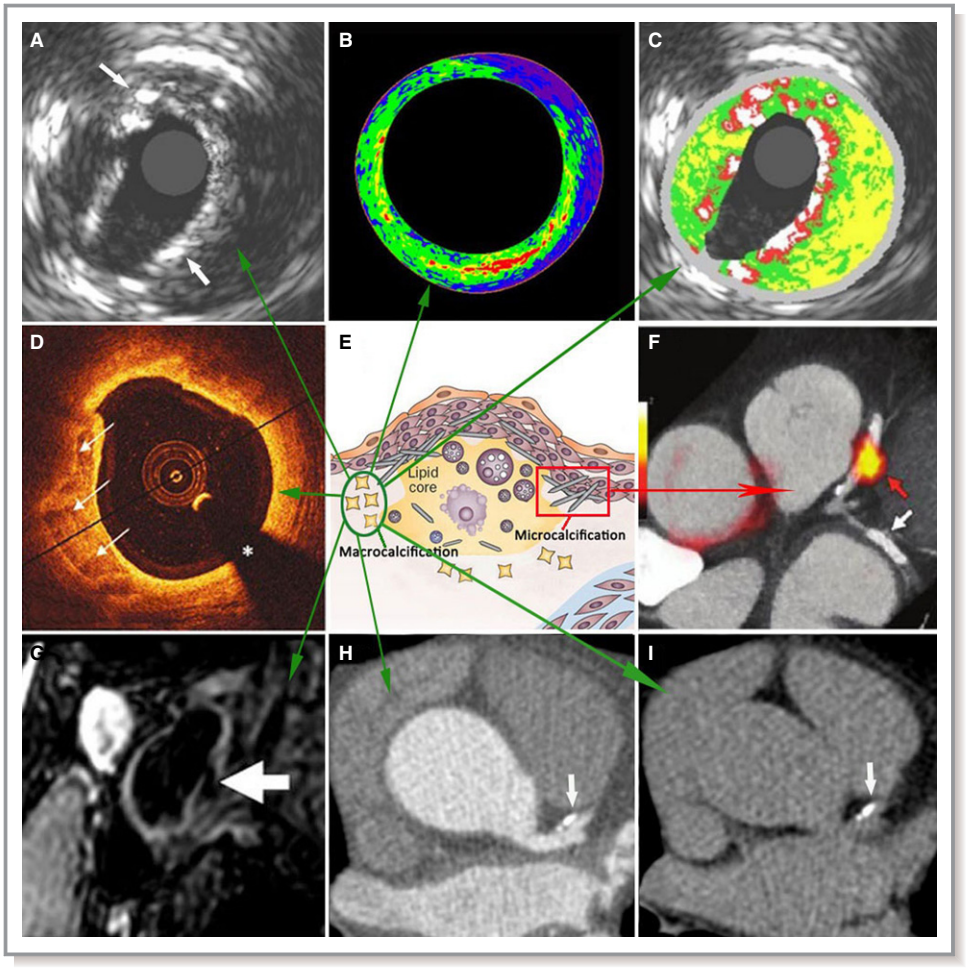

Figure 2. Multimodality imaging of cardiovascular calcification. Representative illustration of current and emerging calcification imaging multimodalities. Each modality offers unique measurements of calcification. Together, they offer the molecular, anatomical, and functional imaging of calcification, which can be used to make sense of current calcific activity, the procession of atherosclerosis, and overall disease burden in patients. A, Grayscale intravascular ultrasound (IVUS) image demonstrating a heavily calcified plaque. B, Integrated backscatter-IVUS image demonstrating 2-dimensional color-coded map (red: calcification, yellow: dense fibrosis, green: fibrosis, blue and purple: lipid pool). C, Virtual histology IVUS image demonstrating coronary plaque with dense calcifications (white color) with corresponding grayscale IVUS image. D, Optical coherence tomography (OCT) image demonstrating coronary arterial calcification (arrows indicate well-demarcated calcification). E, Pathogenic processes demonstrating the atherosclerotic plaque, including lipid core and calcification. Two forms of calcification can be seen: microcalcification and macrocalcification. Each form of calcification is linked with a related visual imaging modality. Green arrows link macrocalcification with many imaging techniques (including computed tomography [CT], magnetic resonance imaging [MRI], [IVUS], and [OCT]), which can visualize the macrocalcification in plaque, whereas the red arrow links microcalcification with the ^{18}F-NaF positron emission tomography (PET) imaging technique, which can visualize the microcalcification in plaque. F, ^{18}F-NaF (PET)–CT image demonstrating high tracer uptake (red arrow) in the left anterior descending artery culprit lesion revealing active plaque microcalcification and no tracer uptake (white arrow) in the nonculprit lesion. G, Three-dimensional (3D) Isotropic-Resolution Black-Blood MRI (3D-MERGE) image demonstrating clearly calcification of right carotid plaque (arrow). H, Transverse contrast-enhanced coronary CT angiography image demonstrating an area of calcium (white arrow) in the left anterior descending coronary artery. I, Non-contrast-enhanced calcium scoring image demonstrating an area of calcium (white arrow) in the left anterior descending coronary artery. A and C, Reprinted from van Velzen et al[18] with permission. Copyright ©2011, Wiley. B, Reprinted from Kawasaki et al[19] with permission. Copyright ©2015, MDPI AG, Basel, Switzerland. D, Reprinted from Batty et al[20] with permission. Copyright ©2016, Wiley. E, Reprinted from Tarkin et al[21] with permission. Copyright ©2014, Wiley. F, Reprinted from Joshi et al[22] with permission. Copyright ©2014, Elsevier Inc. G, Reprinted from Balu et al[23] with permission Copyright ©2010, Wiley.

unit, as is commonly conceived, and patterns of CAC (eg, spotty calcification versus more coalesced calcification) or its density may have different meanings than the lone number (the Agatston CAC score).[60]

Relative advantages of CACS performed by non-contrast-enhanced CT include ease of performance and interpretation, high reproducibility, low cost, and a lack of need for an intravenous contrast agent.[61] However, there are important limitations of CACS including that it generally only represents ≈20% of total plaque volume, it cannot be used to determine if there is flow-limiting stenosis, and it does not provide information on plaque morphology or subtype because of its lower resolution and poor tissue contrast.[62] CACS CT imaging is also unable to detect calcification accurately at a molecular level[33] and does not discriminate between microcalcification and macrocalcification, potential markers of vulnerable and stable atherosclerotic plaques, respectively.[63,64]

Contrast-enhanced coronary CT angiography scans offer improved resolution and tissue contrast, which facilitate an improved evaluation of coronary anatomy and allow an assessment of the severity of luminal stenoses. Moreover, this technique provides information about the morphology and composition of plaques, including high-risk features such as low-attenuation plaque, spotty calcification, and "napkin-ring" sign.[65,66] Spotty calcification—the presence of small, scattered foci of calcium (≤3 mm in diameter) —presents a higher risk of plaque rupture in comparison to single, large deposits of the same total cross-sectional area,[67] and is more frequently observed in the culprit lesions of patients with acute coronary syndrome.[57,65] However, contrast-enhanced coronary CT angiography is limited by the presence of iodine in contrast media, which makes it difficult to precisely identify and quantify CACS.[61]

In summary, multidetector CT is a useful first-line diagnostic technique to estimate the macrocalcification burden. Nonetheless, detection of microcalcification is not possible with clinical CT systems because of their low sensitivity and resolution. Nevertheless, current clinical guidelines suggest using noncontrast CT imaging for CACS to provide clinical risk assessment in appropriate asymptomatic patients and to support the use of CAC screening to guide statin treatment decisions in some patients.[68]

Magnetic Resonance Imaging

Since 1985, magnetic resonance angiography has been used in clinics.[69] Cardiac magnetic resonance angiography allows for a noninvasive assessment of the coronary anatomy without exposing patients to radiation, with excellent soft tissue resolution, and is superior to contrast-enhanced coronary CT angiography for the evaluation of luminal narrowing in heavily calcified coronary segments.[70]

However, vascular calcification is diamagnetic and with only a few protons present, visualization is poor with conventional MRI sequences.[71,72] In past decades, there has been considerable progress in MR scanning technology and parameters, including the development of multicontrast MR protocols.[73–75] Furthermore, image acquisition time, success rate, the demonstration of calcification, and the diagnostic accuracy of cardiac magnetic resonance angiography have all steadily improved.[76–80]

However, assessment of the coronary arteries by cardiac magnetic resonance is still challenging, because of the small size of the vessels, prolonged acquisition time, and complex motions caused by cardiac contractions and respiration.[81] The carotid artery is large, superficial, and clinically important as a major source of ischemic stroke. Moreover, the carotid arteries can be imaged using phased-array coils and well-tested multicontrast imaging protocols such as bright- and black-blood techniques.[82] All of these make the carotid artery the most commonly assessed vessel in MRI studies of atherosclerosis.[23,83–85]

Fabiano et al[86] investigated the utility of multicontrast MRI in identifying calcified carotid plaque with an accuracy and specificity of 98% and 99%, respectively. Moreover, Mujaj et al[87] compared CT- and cardiac magnetic resonance–based volumes of carotid artery calcification and established that they were highly correlated with each other. However, cardiac magnetic resonance–based calcification is systematically smaller than those obtained by CT. Despite this difference, both modalities provided comparable clinical information about a history of stroke. The study of Yang et al[88] also demonstrated that the calcification seen in multidetetor computed tomography (MDCT) is clearly depicted in MRI images at the same location and with roughly the same size in the femoral artery. Baheza et al[89] thought that cardiac magnetic resonance underestimated the amount of calcification, because a certain amount of calcification is required before the MR signal disappears, and possible microcalcification in the atherosclerotic plaque may be missed.

All of the morphologic calcific imaging techniques described above provide an assessment of the information on the extent, density, and its spatial distribution of calcification in plaque, but are unable to identify the active process of calcification in plaque.[90]

Positron Emission Tomography

Feasibility of Evaluating Vascular Calcification Using ^{18}F-NaF Positron Emission Tomography

^{18}F-sodium fluoride (^{18}F-NaF) is a bone tracer that has been used to detect novel areas of bone formation and remodeling since the 1960s.[91,92] The radiotracer binds and incorporates

onto the surface of hydroxyapatite crystals by exchanging with hydroxyl ions to form the fluoroapatite.[64,93] Although the most commonly implemented clinical nuclear bone tracer is a technetium-based radiotracer compound that is imaged with single photon emission computed tomography, ^{18}F-NaF has superior characteristics for bone imaging because of the improved resolution of positron emission tomography (PET) in comparison to single photon emission computed tomography.

The biology of the formation and progression of vascular calcification is similar to that in bone formation. Hydroxyapatite crystals in the vessel wall share histological findings with ectopically formed bone (eg, the presence of osteoclast-like and osteoblast-like cells).[94] Early pathologic studies also observed that arterial calcification resembles a focus of skeleton-like tissue.[95] Additionally, Jeziorska et al observed that the arterial calcification microenvironment has a histochemical resemblance to areas of osteogenesis and bone remodeling (eg, the foci of osteoid matrix, osteocytes, and thin bone trabeculae).[96] Modern histopathologic research further confirmed this hypothesis and demonstrated that cells in areas of vascular calcification are derived from osteoclastic and osteoblastic cells.[97,98]

Recently, substantial attention has been given to using ^{18}F-NaF to investigate vascular calcification in the coronary arteries,[22,64] the aorta,[99] and the carotid arteries,[100] and it has rapidly gained acceptance as a useful tool for the investigation of plaque pathobiology.

Irkle et al[17] studied the mechanism of ^{18}F-NaF vascular uptake by performing comprehensive examinations of carotid artery plaques in vivo and in vitro. In this study, pharmacodynamic and pharmacokinetic analysis confirmed the beneficial properties of ^{18}F-NaF for plaque assessment (eg, high affinity for calcification, stability before scanning, low plasma activity at the time of scanning with minimal myocardial uptake) and showed that the tracer is more specific to microcalcification than macrocalcification.

Several other studies have reported similar findings and have led to growing support for the use of ^{18}F-NaF for imaging the process of microcalcification and visualizing ongoing mineral deposition within the atherosclerotic plaque.[64,99–103]

Divergence Between ^{18}F-NaF Uptake and Calcification Visible on CT

A key realization came from the observation that ^{18}F-NaF PET imaging and CT provided divergent information about atherosclerotic plaques. Dweck et al[64] observed that in spite of a strong correlation between ^{18}F-NaF uptake and CACS (r=0.652, P<0.001), there was no corresponding ^{18}F-NaF uptake in many of the densely calcified regions on CT. In fact, 41% of patients with CACS >1000 had no significant ^{18}F-NaF uptake, and often ^{18}F-NaF uptake was found in areas adjacent to and remote from existing coronary calcification. In a separate study, visible arterial calcium was not associated with higher ^{18}F-NaF uptake, and ^{18}F-NaF uptake was similar in the arterial segments with or without visible calcification.[100] Further investigation into the relationship between ^{18}F-NaF uptake, visible calcification on CT, and the Framingham risk score for CVD showed that ^{18}F-NaF uptake was significantly associated with many cardiovascular risk factors, while visible calcification correlated with age but not other determinants of cardiovascular risk.[104]

Furthermore, an inverse correlation between the plaque calcium density and ^{18}F-NaF uptake was observed by Fiz et al.[105] In this study, they classified plaque calcium density into tertiles: light (130–210 HU), medium (211–510 HU), and heavy (>510 HU). The accumulation of ^{18}F-NaF ebbed in heavier calcific concretions, to a degree that the uptake of ^{18}F-NaF in heavy calcified plaque did not differ from that in control segments. Conversely, the accumulation of ^{18}F-NaF was observed in the arterial segments without calcified plaque in most patients.

The mismatch pattern between CT calcium imaging and ^{18}F-NaF PET imaging occurs as a result of the dynamic and complex procession of vascular calcification.[100,101] In the earliest stage of atherosclerosis, inflammation induces the release of several bone-forming peptides and further promotes the active deposition of hydroxyapatite matrix. The exposed hydroxyapatite crystal surface area in the arterial wall and early active vascular calcification is below the resolution of CT, but the evolving powdery microcalcification is readily identified by ^{18}F-NaF (Figure 3).[22,98,106] Dweck et al[106] investigated histological markers of active calcification (ie, tissue nonspecific alkaline phosphatase and osteocalcin) in aortic stenosis and found a strong correlation between ^{18}F-NaF uptake and these markers, thus confirming that ^{18}F-NaF PET imaging provides information about the activity of calcification and might differentiate biologically active calcification from stable calcification. Alizarin Red staining also confirmed ^{18}F-NaF uptake in areas of microcalcification[17] (Figure 4). As calcium density gradually increases and becomes quiescent without further precipitation of extracellular calcium,[107] it becomes visible on CT imaging,[108] and its hydroxyapatite core becomes hidden from ^{18}F-NaF.[106] These 2 imaging techniques might represent 2 different but complementary markers of atherosclerotic calcification.[105]

Evaluation of Calcification by ^{18}F-NaF PET as a Predictor of Plaque Rupture and Cardiovascular Risk

Ruptured atherosclerotic plaque may lead to adverse CVD events such as acute myocardial infarction or stroke.

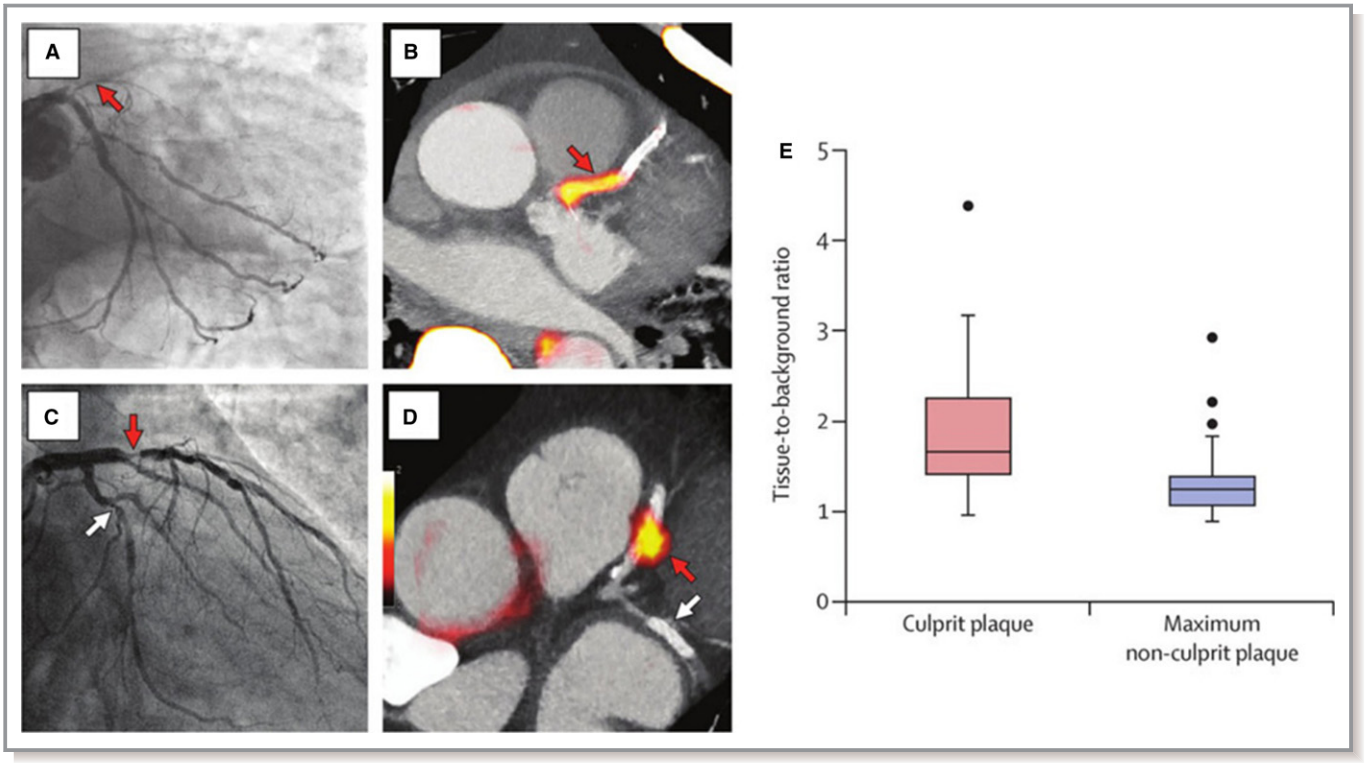

Figure 3. ^{18}F-NaF uptake is increased in coronary artery culprit lesions. Joshi et al evaluated ^{18}F-NaF uptake in the coronary arteries, using positron emission tomography/computed tomography (PET/CT) imaging in the coronary arteries in individuals who had a recent myocardial infarction. A red arrow marks the site of severe stenosis, which is the culprit lesion (left anterior descending artery), while a white arrow marks the site of severe stenosis, which is a bystander non-culprit lesion (circumflex artery) on invasive coronary angiography for 2 patients (A and C). ^{18}F-NaF PET imaging in those same individuals (B and D) shows intense ^{18}F-NaF activity at the site of the culprit left anterior descending artery lesions, but at the site of non-culprit lesions, the CT image demonstrates obvious calcification, whereas there is no ^{18}F-NaF activity at this site. Group mean data (E) demonstrate that ^{18}F-fluoride activity in the culprit lesions is higher than that in non-culprit vessels. Reprinted from Joshi et al[22] with permission. Copyright ©2014, Elsevier Inc.

Microcalcification increases the risk of plaque rupture by increasing mechanical wall stress and predisposing the plaque to microfractures and subsequent thrombosis.[4,13,67]

Growing evidence supports the utility of ^{18}F-NaF PET imaging for the evaluation of the risk associated with atherosclerotic plaques. A prospective clinical study[22] provides a robust and cogent argument that ^{18}F-NaF uptake detects coronary artery microcalcification and identifies vulnerable and high-risk plaques in patients with acute myocardial infarction and stable angina. In patients with myocardial infarction, the ^{18}F-NaF uptake in 93% of culprit plaques was significantly higher than that in nonculprit plaques. Furthermore, pathological evidence from plaques excised during carotid endarterectomy verified the fact that marked ^{18}F-NaF uptake occurred at the site of all carotid plaque ruptures and was associated with histological evidence of active calcification, macrophage infiltration, apoptosis, and necrosis. In patients with stable angina, 45% of patients had plaques with focal ^{18}F-NaF uptake that were associated with more high-risk features on intravascular ultrasound than those without uptake, including positive remodeling, microcalcification, and necrotic core. Likewise, Vesey et al[109] performed ^{18}F-NaF PET/CT in patients after recent transient ischemic attack or minor ischemic stroke and found that carotid ^{18}F-NaF uptake was increased in culprit plaques in comparison with asymptomatic contralateral plaques and correlated with CVD risk.

^{18}F-NaF PET imaging has also been shown to provide a useful method of predicting changes in plaque calcification. Dweck et al[106] observed that baseline ^{18}F-NaF uptake in stenotic aortic valves provides a marker of active calcification that correlated closely with change in calcium score (r=0.66, P<0.01) and predicted the change in valvular CT calcium scores at 1 year. Jenkins et al[110] also investigated the value of valvular ^{18}F-NaF uptake in predicting disease progression and clinical outcome in patients with aortic stenosis. The results demonstrated that baseline ^{18}F-fluoride uptake correlated strongly with the subsequent rate of progression in aortic valve calcium score and independently predicts cardiovascular death and aortic valve replacement after age and sex adjustments (hazard ratio: 1.55; 95% CI, 1.33–1.81; P<0.001). Furthermore, Beheshti et al[98] found

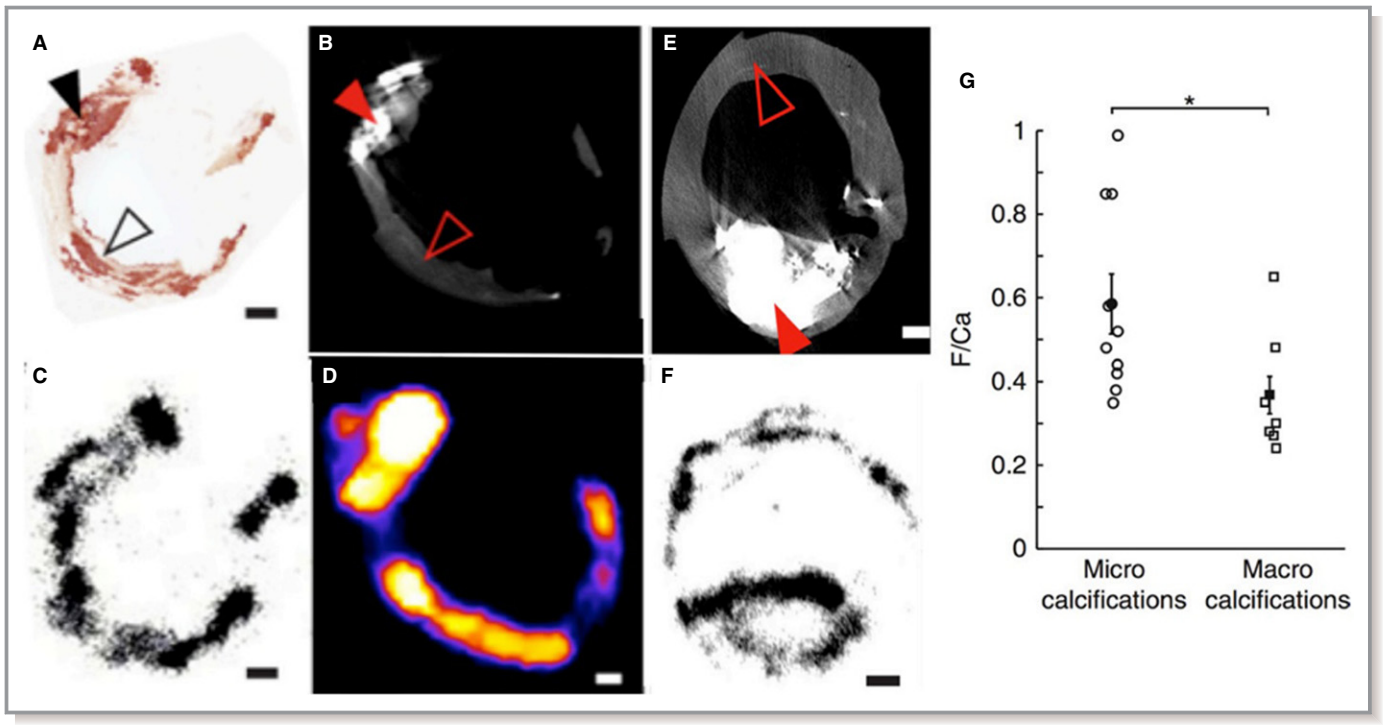

Figure 4. ^{18}F-Fluoride preferentially binds microcalcification beyond the resolution of computed tomography (CT). Images are taken ex vivo of a carotid endarterectomy specimen excised from a patient who had a recent stroke. A, Histological section of the excised plaque stained for calcium with Alizarin red. B, Filled black arrow shows an area of dense macroscopic calcification that is visible on micro-CT. By comparison, the empty black arrowhead demonstrates areas of microcalcification that are beyond the resolution of the micro-CT but by comparison demonstrate avid binding with ^{18}F-NaF on both autoradiography (C) and micro–positron emission tomography imaging (D). E, A second carotid endarterectomy sample from a patient post stroke demonstrates a large macrocalcific deposit on micro-CT. F, Autoradiography shows that although ^{18}F-NaF is able to bind to the surface of the plaque, it is unable to penetrate into the center. G, The amount of fluoride adsorbed to microcalcifications is significantly higher than macrocalcifications (F/Ca ratio in microcalcifications 0.59±0.23 (n=10, individual plaques) ; in macrocalcifications 0.37±0.15 (n=7, individual plaques)); *P<0.02 using an ANOVA and Tukey Kramer *post hoc* test. As a consequence of this effect, ^{18}F-NaF binds preferentially to regions of microcalcification compared with macroscopic deposits. Reprinted from Irkle et al[17] with permission. Copyright ©2015, Nature Publishing Group, a division of Macmillan Publishers Limited.

that ^{18}F-NaF PET/CT allowed the detection of early molecular and cellular calcification in atherosclerotic plaque and may provide highly relevant information about the state of calcified plaque before macroscopic calcification can be detectable by standard CT techniques. These findings suggest that this modality may allow earlier risk stratification and therapeutic intervention in patients with asymptomatic atherosclerosis.

Additional research has shown that patients with increased ^{18}F-NaF uptake were more likely to have a clinical diagnosis of coronary artery disease, anginal symptoms, and a higher burden of systemic atherosclerosis. Ten-year Framingham risk scores for CVD and death are related to ^{18}F-NaF uptake.[64] Other retrospective studies have shown positive correlations between arterial ^{18}F-NaF uptake and CVD risk factors, including age, sex, hypertension, hypercholesterolemia, and diabetes mellitus, further supporting the notion that ^{18}F-NaF PET imaging may improve CVD risk stratification.[98,100–102,104,111–114]

In summary, ^{18}F-NaF PET imaging has been shown to be useful for the identification of early active calcification and microcalcification.[105] This factor makes it potentially useful for the identification of vulnerable plaque[115] and individuals with high CVD risk.[22,64,116]

Limitations of ^{18}F-NaF PET Imaging

^{18}F-NaF PET imaging has lower spatial resolution than CT imaging and continuous cardiac motion, which may prevent accurate quantification of coronary artery microcalcification. However, Dweck et al[64] have reported that the spatial resolution of ^{18}F-NaF PET was sufficient to allow location of culprit lesions in coronary territories, and continuous cardiac movement can be addressed by using gating. Furthermore, even if the small size of the coronary arteries may fall below the resolution of most PET scanners[117] and leads to underestimation of the PET signal because of a partial volume effect, Beheshti et al[102] proposed that ^{18}F-NaF deposition could be measured throughout the entire myocardium, including a semiquantitative analysis of the contribution from both the major vessels and the microvasculature, in order to

limit the impact of smear artifacts caused by the cardiac motion and small vessel diameter. They also emphasized excluding the aortic valve from the region of interest to avoid contamination by the aortic wall or calcified aortic valve leaflets.

Alternative PET Imaging Tracers

Published studies[10,118] have evaluated the association between arterial calcification and inflammation of vascular disease and demonstrated that in early-stage atherosclerosis, inflammation precedes calcification, and macrophages promote the proinflammatory milieu and send specific signals to vascular wall cells to initiate osteogenic differentiation. Then, both processes developed in parallel and within close proximity. Microcrystals of calcium phosphate may elicit proinflammatory responses from macrophages and build a positive-feedback amplification loop of calcification and inflammation that drives disease progression. In addition, macrophages and smooth muscle cells may undergo apoptotic changes, providing new foci for calcium deposition. Thus, the evaluation of inflammation is also very important to better understand the process of calcification and atherosclerotic plaques.

^{18}F-2-Deoxy-2-fluoro-D-glucose (^{18}F-FDG) is the most widely validated PET tracer for the evaluation of inflammation within atherosclerotic plaques on the basis of the glucose metabolism of macrophages.[21] Li et al[119] used ^{18}F-NaF and ^{18}F-FDG PET/CT to evaluate the association between osteogenesis and inflammation during the progression of calcified plaque. They observed that early atherosclerotic osteogenesis is determined by macrophage accumulation and further intensive progression of arterial calcification might be associated with reduced inflammation. Furthermore, ^{18}F-FDG PET/CT can provide additional diagnostic and prognostic information beyond anatomic imaging alone.[120] It is becoming increasingly evident that ^{18}F-FDG PET/CT is capable of quantifying atherosclerotic inflammation and predicting subsequent cardiovascular events[121] and providing a means of evaluating changes with treatment.[122] Nevertheless, ^{18}F-FDG lacks cell specificity, and in contrast to ^{18}F-NaF, is extremely limited for the assessment of coronary arteries because of myocardial spillover in spite of significant efforts at background myocardial suppression.[22]

In atherosclerotic inflammation, the surface of activated macrophages overexpresses the G-protein-coupled receptor somatostatin receptor subtype-2.[123] Preclinical[124] and retrospective[125,126] studies suggest that gallium-68-labeled [1,4,7,10-tetraazacy-clododecane-*N*,*N*′,*N*″,*N*‴-tetraacetic acid]-D-Phe1, Tyr3-octreotate (DOTATATE), a somatostatin receptor subtype-2-binding PET tracer, may be superior to ^{18}F-FDG for imaging atherosclerotic inflammation. Tarkin et al[127] validated ^{68}Ga-DOTATATE PET as a novel marker of atherosclerotic inflammation and showed that ^{68}Ga-DOTATATE PET offers superior coronary imaging, excellent macrophage specificity, and better power to discriminate high-risk versus low-risk coronary lesions than ^{18}F-FDG. These findings require confirmation in larger studies, and the utility of ^{68}Ga-DOTATATE PET in the prediction of clinical outcomes should be tested.

Notably, neither ^{18}F-FDG nor ^{68}Ga-DOTATATE PET is able to evaluate vascular microcalcification.

Intravascular Imaging

Invasive angiography offers superior spatial resolution (0.1–0.2 mm) and temporal resolution (10 ms) and has been the criterion standard for coronary atherosclerosis imaging for more than 50 years.[128] It generates a 2-dimensional silhouette of the arterial lumen and does not image the vessel wall; thus, it does not provide direct imaging of calcification or the atherosclerotic plaque itself.

With ultrasound techniques (eg, vascular, transesophageal, and intravascular ultrasound [IVUS]), it is possible to directly image the vessel wall and analyze atherosclerotic plaques in various arterial beds including the carotids, aorta, and coronary arteries. It also allows monitoring of the natural history of plaque formation and identification of the compositional features. Usually, atherosclerotic plaque may appear in 3 distinct textural patterns by parameters of acoustic attenuation[129]: hypoechoic (lipid-rich or hemorrhagic plaque), moderately hyperechoic (fibrotic or fibrofatty plaque), and markedly hyperechoic with shadowing (calcific plaque). Hyperechoic calcified plaque is easily identified by its strongly reflective ultrasound properties with an attenuation 700% greater than that in normal wall and 300% greater than that in atherosclerotic noncalcific plaques. Alternatively, hypoechoic plaque shows poor or no reflection.[130,131]

Grayscale IVUS uses miniaturized crystals and generates high-resolution images of the vessel wall and lumen to allow quantitative measurements to the plaque area, but its limited axial resolution (150 μm) and lateral resolution (300 μm) render it unable to differentiate individual plaque components.[132]

Virtual histology IVUS, an advanced radiofrequency analysis of reflected ultrasound signals, allows reconstruction of a color-coded tissue map, and provides an improved assessment of plaque composition including necrotic, fibrous, densely calcified, and fibrofatty regions with reasonable accuracy.[133] Nevertheless, it remains limited by noise, artifacts, and insufficient spatial resolution.[134]

Integrated backscatter intravascular ultrasound (IB-IVUS) is another promising technique. In this technique, IB values for each tissue component are calculated as the average power using a fast Fourier transform, an algorithm that samples a signal over a period of time or space and divides it into its

frequency components. These components are single sinusoidal oscillations at distinct frequencies with their own amplitudes and phases that are measured as decibels of the frequency component of the backscattered signal from a small volume of tissue. In IB-IVUS images, color-coded maps have 4 major components based on different radiofrequency signals: fibrosis (green), dense fibrosis (yellow), lipid (blue), and calcification (red). Kawasaki et al[135] demonstrated that IB-IVUS depicts calcified lesions with high sensitivity. However, a limitation resides in the fact that very dense fibrous lesions may produce sufficient reflectivity and attenuation or acoustic shadowing to be misclassified as calcified.[136] Furthermore, Okubo et al[137] showed that IB-IVUS occasionally underestimated calcified lesions and overestimated lipid pools behind calcifications as a consequence of the acoustic shadowing resulting from the calcification. Moreover, the ability to detect ultrasonically hypoechoic microcalcification with IB-IVUS is limited.

Other intravascular coronary imaging modalities such as optical coherence tomography have been increasingly evaluated by recent studies. Optical coherence tomography has high spatial resolution (10–15 μm), allows the evaluation of variations in plaque composition at a cellular level, and distinguishes between plaque types.[138] However, correct differentiation between calcium and lipid can be challenging with optical coherence tomography, and its limited tissue penetration (1–3 mm) makes the assessment of the entire plaque volume impossible. Optical frequency domain imaging, a second generation of optical coherence tomography, has shown an ability to discriminate plaque composition that relates to findings at autopsy and quantitatively evaluates the thickness and border of vascular calcification.[139]

Importantly, all of the invasive angiography techniques are limited in their ability to identify microcalcification.

Conclusions

Significant advances have been made in our understanding of the mechanism of atherosclerotic calcification and the value of multimodality imaging techniques for evaluating this pathological process. ^{18}F-NaF PET imaging provides unique information about the pathologic process of vascular calcification and identifies microcalcification, which makes it a promising tool for performing noninvasive, reproducible measurements of active plaque calcification that correlate with vulnerability and culprit plaques. The combination of ^{18}F-NaF PET imaging with other structural imaging modalities (eg, CT) may provide a noninvasive, qualitative, and quantitative assessment of calcification and plaque vulnerability in atherosclerotic disease that offers important diagnostic and prognostic insights for the assessment of CVD risk and the monitoring of clinical treatment.

Acknowledgments

We thank Dr Aluru John Sukumar for providing contrast and noncontrast CT images used in Figure 2.

Sources of Funding

Michael T. Osborne, MD is supported by NIH grant #T32HL076136.

Disclosures

None.

References

1. Hartiala O, Magnussen CG, Kajander S, Knuuti J, Ukkonen H, Saraste A, Rinta-Kiikka I, Kainulainen S, Kähönen M, Hutri-Kähönen N, Laitinen T, Lehtimäki T, Viikari JS, Hartiala J, Juonala M, Raitakari OT. Adolescence risk factors are predictive of coronary artery calcification at middle age: the Cardiovascular Risk in Young Finns Study. *J Am Coll Cardiol*. 2012;60:1364–1370.
2. Abdelbaky A, Corsini E, Figueroa AL, Fontanez S, Subramanian S, Ferencik M, Brady TJ, Hoffmann U, Tawakol A. Focal arterial inflammation precedes subsequent calcification in the same location: a longitudinal FDG-PET/CT study. *Circ Cardiovasc Imaging*. 2013;6:747–754.
3. Hayden MR, Tyagi SC, Kolb L, Sowers JR, Khanna R. Vascular ossification–calcification in metabolic syndrome, type 2 diabetes mellitus, chronic kidney disease, and calciphylaxis-calcific uremic arteriolopathy: the emerging role of sodium thiosulfate. *Cardiovasc Diabetol*. 2005;4:4.
4. Vengrenyuk Y, Carlier S, Xanthos S, Cardoso L, Ganatos P, Virmani R, Einav S, Gilchrist L, Weinbaum S. A hypothesis for vulnerable plaque rupture due to stress-induced debonding around cellular microcalcifications in thin fibrous caps. *Proc Natl Acad Sci USA*. 2006;103:14678–14683.
5. Genders TS, Pugliese F, Mollet NR, Meijboom WB, Weustink AC, van Mieghem CA, de Feyter PJ, Hunink MG. Incremental value of the CT coronary calcium score for the prediction of coronary artery disease. *Eur Radiol*. 2010;20:2331–2340.
6. Thilo C, Gebregziabher M, Mayer FB, Zwerner PL, Costello P, Schoepf UJ. Correlation of regional distribution and morphological pattern of calcification at CT coronary artery calcium scoring with non- calcified plaque formation and stenosis. *Eur Radiol*. 2010;20:855–861.
7. Budoff MJ, Shaw LJ, Liu ST, Weinstein SR, Mosler TP, Tseng PH, Flores FR, Callister TQ, Raggi P, Berman DS. Long-term prognosis associated with coronary calcification: observations from a registry of 25, 253 patients. *J Am Coll Cardiol*. 2007;49:1860–1870.
8. Hou ZH, Lu B, Gao Y, Jiang SL, Wang Y, Li W, Budoff MJ. Prognostic value of coronary CT angiography and calcium score for major adverse cardiac events in outpatients. *JACC Cardiovasc Imaging*. 2012;5:990–999.
9. Ley K, Miller YI, Hedrick CC. Monocyte and macrophage dynamics during atherogenesis. *Arterioscler Thromb Vasc Biol*. 2011;31:1506–1516.
10. Nadra I, Mason JC, Philippidis P, Florey O, Smythe CD, McCarthy GM, Landis RC, Haskard DO. Proinflammatory activation of macrophages by basic calcium phosphate crystals via protein kinase C and MAP kinase pathways: a vicious cycle of inflammation and arterial calcification? *Circ Res*. 2005;96:1248–1256.
11. Lanzer P, Boehm M, Sorribas V, Thiriet M, Janzen J, Zeller T, St Hilaire C, Shanahan C. Medial vascular calcification revisited: review and perspectives. *Eur Heart J*. 2014;35:1515–1525.
12. Sanz J, Fayad ZA. Imaging of atherosclerotic cardiovascular disease. *Nature*. 2008;451:953–957.
13. Hutcheson JD, Maldonado N, Aikawa E. Small entities with large impact: microcalcifications and atherosclerotic plaque vulnerability. *Curr Opin Lipidol*. 2014;25:327–332.
14. Kelly-Arnold A, Maldonado N, Laudier D, Aikawa E, Cardoso L, Weinbaum S. Revised microcalcification hypothesis for fibrous cap rupture in human coronary arteries. *Proc Natl Acad Sci USA*. 2013;110:10741–10746.
15. Ritman EL. Small-animal CT: its difference from, and impact on, clinical CT. *Nucl Instrum Methods Phys Res A*. 2007;580:968–970.
16. Dweck MR, Aikawa E, Newby DE, Tarkin JM, Rudd JH, Narula J, Fayad ZA. Noninvasive molecular imaging of disease activity in atherosclerosis. *Circ Res*. 2016;119:330–340.

17. Irkle A, Vesey AT, Lewis DY, Skepper JN, Bird JL, Dweck MR, Joshi FR, Gallagher FA, Warburton EA, Bennett MR, Brindle KM, Newby DE, Rudd JH, Davenport AP. Identifying active vascular microcalcification by (18)F-sodium fluoride positron emission tomography. *Nat Commun*. 2015;6:7495.
18. van Velzen JE, de Graaf FR, de Graaf MA, Schuijf JD, Kroft LJ, de Roos A, Reiber JH, Bax JJ, Jukema JW, Boersma E, Schalij MJ, van der Wall EE. Comprehensive assessment of spotty calcifications on computed tomography angiography: comparison to plaque characteristics on intravascular ultrasound with radiofrequency backscatter analysis. *J Nucl Cardiol*. 2011;18:893–903.
19. Kawasaki M. An integrated backscatter ultrasound technique for the detection of coronary and carotid atherosclerotic lesions. *Sensors (Basel)*. 2015;15:979–994.
20. Batty JA, Subba S, Luke P, Gigi LW, Sinclair H, Kunadian V. Intracoronary imaging in the detection of vulnerable plaques. *Curr Cardiol Rep*. 2016;18:28.
21. Tarkin JM, Joshi FR, Rudd JH. PET imaging of inflammation in atherosclerosis. *Nat Rev Cardiol*. 2014;11:443–457.
22. Joshi NV, Vesey AT, Williams MC, Shah AS, Calvert PA, Craighead FH, Yeoh SE, Wallace W, Salter D, Fletcher AM, van Beek EJ, Flapan AD, Uren NG, Behan MW, Cruden NL, Mills NL, Fox KA, Rudd JH, Dweck MR, Newby DE. 18F-fluoride positron emission tomography for identification of ruptured and high-risk coronary atherosclerotic plaques: a prospective clinical trial. *Lancet*. 2014;383:705–713.
23. Balu N, Yarnykh VL, Chu B, Wang J, Hatsukami T, Yuan C. Carotid plaque assessment using fast 3D isotropic resolution black-blood MRI. *Magn Reson Med*. 2011;65:627–637.
24. Becker CR, Knez A, Ohnesorge B, Schoepf UJ, Flohr T, Bruening R, Haberl R, Reiser MF. Visualization and quantification of coronary calcifications with electron beam and spiral computed tomography. *Eur Radiol*. 2000;10:629–635.
25. Agatston AS, Janowitz WR, Hildner FJ, Zusmer NR, Viamonte M Jr, Detrano R. Quantification of coronary artery calcium using ultrafast computed tomography. *J Am Coll Cardiol*. 1990;15:827–832.
26. Ichii M, Ishimura E, Shima H, Ohno Y, Ochi A, Nakatani S, Tsuda A, Ehara S, Mori K, Fukumoto S, Naganuma T, Takemoto Y, Nakatani T, Inaba M. Quantitative analysis of abdominal aortic calcification in CKD patients without dialysis therapy by use of the Agatston score. *Kidney Blood Press Res*. 2013;38:196–204.
27. Oudkerk M, Stillman AE, Halliburton SS, Kalender WA, Möhlenkamp S, McCollough CH, Vliegenthart R, Shaw LJ, Stanford W, Taylor AJ, van Ooijen PM, Wexler L, Raggi P. Coronary artery calcium screening: current status and recommendations from the European Society of Cardiac Radiology and North American Society for Cardiovascular Imaging. *Int J Cardiovasc Imaging*. 2008;24:645–671.
28. Kavousi M, Elias-Smale S, Rutten JH, Leening MJ, Vliegenthart R, Verwoert GC, Krestin GP, Oudkerk M, de Maat MP, Leebeek FW, Mattace-Raso FU, Lindemans J, Hofman A, Steyerberg EW, van der Lugt A, van den Meiracker AH, Witteman JC. Evaluation of newer risk markers for coronary heart disease risk classification: a cohort study. *Ann Intern Med*. 2012;156:438–444.
29. Budoff MJ, Gul KM. Expert review on coronary calcium. *Vasc Health Risk Manag*. 2008;4:315–324.
30. Hecht HS. Coronary artery calcium scanning: past, present, and future. *JACC Cardiovasc Imaging*. 2015;8:579–596.
31. Greenland P, Alpert JS, Beller GA, Benjamin EJ, Budoff MJ, Fayad ZA, Foster E, Hlatky MA, Hodgson JM, Kushner FG, Lauer MS, Shaw LJ, Smith SC Jr, Taylor AJ, Weintraub WS, Wenger NK, Jacobs AK; American College of Cardiology Foundation/ American Heart Association Task Force on Practice Guidelines. 2010 ACCF/AHA guideline for assessment of cardiovascular risk in asymptomatic adults: a report of the American College of Cardiology Foundation/American Heart Association Task Force on Practice Guidelines. *Circulation*. 2010;122:e584–e636.
32. Polonsky TS, McClelland RL, Jorgensen NW, Bild DE, Burke GL, Guerci AD, Greenland P. Coronary artery calcium score and risk classification for coronary heart disease prediction. *JAMA*. 2010;303:1610–1616.
33. McEvoy JW, Blaha MJ, Defilippis AP, Budoff MJ, Nasir K, Blumenthal RS, Jones SR. Coronary artery calcium progression: an important clinical measurement? A review of published reports. *J Am Coll Cardiol*. 2010;56:1613–1622.
34. Detrano R, Guerci AD, Carr JJ, Bild DE, Burke G, Folsom AR, Liu K, Shea S, Szklo M, Bluemke DA, O'Leary DH, Tracy R, Watson K, Wong ND, Kronmal RA. Coronary calcium as a predictor of coronary events in four racial or ethnic groups. *N Engl J Med*. 2008;358:1336–1345.
35. Shah S, Bellam N, Leipsic J, Berman DS, Quyyumi A, Hausleiter J, Achenbach S, Al-Mallah M, Budoff MJ, Cademartiri F, Callister TQ, Chang HJ, Chow BJ, Cury RC, Delago AJ, Dunning AL, Feuchtner GM, Hadamitzky M, Karlsberg RP, Kaufmann PA, Lin FY, Chinnaiyan KM, Maffei E, Raff GL, Villines TC, Gomez MJ, Min JK, Shaw LJ; CONFIRM (COronary CT Angiography EvaluatioN For Clinical Outcomes: An InteRnational Multicenter Registry) Investigators. Prognostic significance of calcified plaque among symptomatic patients with nonobstructive coronary artery disease. *J Nucl Cardiol*. 2014;21:453–466.
36. Mori H, Torii S, Kutyna M, Sakamoto A, Finn AV, Virmani R. Coronary artery calcification and its progression: what does it really mean? *JACC Cardiovasc Imaging*. 2018;11:127–142.
37. Sarwar A, Shaw LJ, Shapiro MD, Blankstein R, Hoffmann U, Cury RC, Abbara S, Brady TJ, Budoff MJ, Blumenthal RS, Nasir K. Diagnostic and prognostic value of absence of coronary artery calcification. *JACC Cardiovasc Imaging*. 2009;2:675–688.
38. Puri R, Nicholls SJ, Shao M, Kataoka Y, Uno K, Kapadia SR, Tuzcu EM, Nissen SE. Impact of statins on serial coronary calcification during atheroma progression and regression. *J Am Coll Cardiol*. 2015;65:1273–1282.
39. Nakahara T, Dweck MR, Narula N, Pisapia D, Narula J, Strauss HW. Coronary artery calcification: from mechanism to molecular imaging. *JACC Cardiovasc Imaging*. 2017;10:582–593.
40. Leber AW, Knez A, White CW, Becker A, von Ziegler F, Muehling O, Becker C, Reiser M, Steinbeck G, Boekstegers P. Composition of coronary atherosclerotic plaques in patients with acute myocardial infarction and stable angina pectoris determined by contrast-enhanced multislice computed tomography. *Am J Cardiol*. 2003;91:714–718.
41. Shemesh J, Apter S, Itzchak Y, Motro M. Coronary calcification compared in patients with acute versus in those with chronic coronary events by using dual-sector spiral CT. *Radiology*. 2003;226:483–488.
42. Heart Protection Study Collaborative Group. MRC/BHF Heart Protection Study of cholesterol lowering with simvastatin in 20,536 high-risk individuals: a randomised placebo-controlled trial. *Lancet*. 2002;360:7–22.
43. Henein M, Granasen G, Wiklund U, Schmermund A, Guerci A, Erbel R, Raggi P. High dose and long-term statin therapy accelerate coronary artery calcification. *Int J Cardiol*. 2015;184:581–586.
44. Terry JG, Carr JJ, Kouba EO, Davis DH, Menon L, Bender K, Chandler ET, Morgan T, Crouse JR III. Effect of simvastatin (80 mg) on coronary and abdominal aortic arterial calcium (from the coronary artery calcification treatment with zocor [CATZ] study). *Am J Cardiol*. 2007;99:1714–1717.
45. Arad Y, Spadaro LA, Roth M, Newstein D, Guerci AD. Treatment of asymptomatic adults with elevated coronary calcium scores with atorvastatin, vitamin C, and vitamin E: the St. Francis Heart Study randomized clinical trial. *J Am Coll Cardiol*. 2005;46:166–172.
46. Raggi P, Davidson M, Callister TQ, Welty FK, Bachmann GA, Hecht H, Rumberger JA. Aggressive versus moderate lipid-lowering therapy in hypercholesterolemic postmenopausal women: Beyond Endorsed Lipid Lowering with EBT Scanning (BELLES). *Circulation*. 2005;112:563–571.
47. Houslay ES, Cowell SJ, Prescott RJ, Reid J, Burton J, Northridge DB, Boon NA, Newby DE; Scottish Aortic Stenosis and Lipid Lowering Therapy, Impact on Regression trial Investigators. Progressive coronary calcification despite intensive lipid-lowering treatment: a randomised controlled trial. *Heart*. 2006;92:1207–1212.
48. Henein MY, Owen A. Statins moderate coronary stenoses but not coronary calcification: results from meta-analyses. *Int J Cardiol*. 2011;153:31–35.
49. Stary HC. The development of calcium deposits in atherosclerotic lesions and their persistence after lipid regression. *Am J Cardiol*. 2001;88:16E–19E.
50. Daoud AS, Jarmolych J, Augustyn JM, Fritz KE. Sequential morphologic studies of regression of advanced atherosclerosis. *Arch Pathol Lab Med*. 1981;105:233–239.
51. Zhao XQ, Yuan C, Hatsukami TS, Frechette EH, Kang XJ, Maravilla KR, Brown BG. Effects of prolonged intensive lipid-lowering therapy on the characteristics of carotid atherosclerotic plaques in vivo by MRI: a case-control study. *Arterioscler Thromb Vasc Biol*. 2001;21:1623–1629.
52. Inoue K, Motoyama S, Sarai M, Sato T, Harigaya H, Hara T, Sanda Y, Anno H, Kondo T, Wong ND, Narula J, Ozaki Y. Serial coronary CT angiography-verified changes in plaque characteristics as an end point: evaluation of effect of statin intervention. *JACC Cardiovasc Imaging*. 2010;3:691–698.
53. Ferreira TS, Lanzetti M, Barroso MV, Rueff-Barroso CR, Benjamim CF, de Brito-Gitirana L, Porto LC, Valença SS. Oxidative stress and inflammation are differentially affected by atorvastatin, pravastatin, rosuvastatin, and simvastatin on lungs from mice exposed to cigarette smoke. *Inflammation*. 2014;37:1355–1365.
54. Takayama T, Hiro T, Ueda Y, Honye J, Komatsu S, Yamaguchi O, Li Y, Yajima J, Takazawa K, Nanto S, Saito S, Hirayama A, Kodama K. Plaque stabilization by intensive LDL-cholesterol lowering therapy with atorvastatin is delayed in type 2 diabetic patients with coronary artery disease-serial angioscopic and intravascular ultrasound analysis. *J Cardiol*. 2013;61:381–386.
55. Pugliese G, Iacobini C, Blasetti Fantauzzi C, Menini S. The dark and bright side of atherosclerotic calcification. *Atherosclerosis*. 2015;238:220–230.

56. Cowell SJ, Newby DE, Prescott RJ, Bloomfield P, Reid J, Northridge DB, Boon NA; Scottish Aortic Stenosis and Lipid Lowering Trial, Impact on Regression (SALTIRE) Investigators. A randomized trial of intensive lipid-lowering therapy in calcific aortic stenosis. *N Engl J Med*. 2005;352:2389–2397.
57. Ehara S, Kobayashi Y, Yoshiyama M, Shimada K, Shimada Y, Fukuda D, Nakamura Y, Yamashita H, Yamagishi H, Takeuchi K, Naruko T, Haze K, Becker AE, Yoshikawa J, Ueda M. Spotty calcification typifies the culprit plaque in patients with acute myocardial infarction: an intravascular ultrasound study. *Circulation*. 2004;110:3424–3429.
58. Criqui MH, Denenberg JO, Ix JH, McClelland RL, Wassel CL, Rifkin DE, Carr JJ, Budoff MJ, Allison MA. Calcium density of coronary artery plaque and risk of incident cardiovascular events. *JAMA*. 2014;311:271–278.
59. Yeboah J, McClelland RL, Polonsky TS, Burke GL, Sibley CT, O'Leary D, Carr JJ, Goff DC, Greenland P, Herrington DM. Comparison of novel risk markers for improvement in cardiovascular risk assessment in intermediate-risk individuals. *JAMA*. 2012;308:788–795.
60. Shaw LJ, Narula J, Chandrashekhar Y. The never-ending story on coronary calcium: is it predictive, punitive, or protective? *J Am Coll Cardiol*. 2015;65:1283–1285.
61. Song I, Yi JG, Park JH, Kim SM, Lee KS, Chung MJ. Virtual non-contrast CT using dual-energy spectral CT: feasibility of coronary artery calcium scoring. *Korean J Radiol*. 2016;17:321–329.
62. Joshi PH, Blaha MJ, Blumenthal RS, Blankstein R, Nasir K. What is the role of calcium scoring in the age of coronary computed tomographic angiography? *J Nucl Cardiol*. 2012;19:1226–1235.
63. Virmani R, Burke AP, Farb A, Kolodgie FD. Pathology of the vulnerable plaque. *J Am Coll Cardiol*. 2006;47(8 suppl):C13–C18.
64. Dweck MR, Chow MW, Joshi NV, Williams MC, Jones C, Fletcher AM, Richardson H, White A, McKillop G, van Beek EJ, Boon NA, Rudd JH, Newby DE. Coronary arterial ^{18}F-sodium fluoride uptake: a novel marker of plaque biology. *J Am Coll Cardiol*. 2012;59:1539–1548.
65. Motoyama S, Kondo T, Sarai M, Sugiura A, Harigaya H, Sato T, Inoue K, Okumura M, Ishii J, Anno H, Virmani R, Ozaki Y, Hishida H, Narula J. Multislice computed tomographic characteristics of coronary lesions in acute coronary syndromes. *J Am Coll Cardiol*. 2007;50:319–326.
66. Maurovich-Horvat P, Hoffmann U, Vorpahl M, Nakano M, Virmani R, Alkadhi H. The napkin-ring sign: CT signature of high-risk coronary plaques? *JACC Cardiovasc Imaging*. 2010;3:440–444.
67. Kataoka Y, Wolski K, Uno K, Puri R, Tuzcu EM, Nissen SE, Nicholls SJ. Spotty calcification as a marker of accelerated progression of coronary atherosclerosis: insights from serial intravascular ultrasound. *J Am Coll Cardiol*. 2012;59:1592–1597.
68. Stone NJ, Robinson JG, Lichtenstein AH, Bairey Merz CN, Blum CB, Eckel RH, Goldberg AC, Gordon D, Levy D, Lloyd-Jones DM, McBride P, Schwartz JS, Shero ST, Smith SC Jr, Watson K, Wilson PW; American College of Cardiology/ American Heart Association Task Force on Practice Guidelines. 2013 ACC/AHA guideline on the treatment of blood cholesterol to reduce atherosclerotic cardiovascular risk in adults: a report of the American College of Cardiology/American Heart Association Task Force on Practice Guidelines. *J Am Coll Cardiol*. 2014;63:2889–2934.
69. Wedeen VJ, Meuli RA, Edelman RR, Geller SC, Frank LR, Brady TJ, Rosen BR. Projective imaging of pulsatile flow with magnetic resonance. *Science*. 1985;230:946–948.
70. Sakuma H. Coronary CT versus MR angiography: the role of MR angiography. *Radiology*. 2011;258:340–349.
71. Wu Z, Mittal S, Kish K, Yu Y, Hu J, Haacke E. Identification of calcification with MRI using susceptibility-weighted imaging: a case study. *J Magn Reson Imaging*. 2009;29:177–182.
72. Chen W, Zhu W, Kovanlikaya I, Kovanlikaya A, Liu T, Wang S, Salustri C, Wang Y. Intracranial calcifications and hemorrhages: characterization with quantitative susceptibility mapping. *Radiology*. 2014;270:496–505.
73. Shinnar M, Fallon JT, Wehrli S, Levin M, Dalmacy D, Fayad ZA, Badimon JJ, Harrington M, Harrington E, Fuster V. The diagnostic accuracy of ex vivo MRI for human atherosclerotic plaque characterization. *Arterioscler Thromb Vasc Biol*. 1999;19:2756–2761.
74. Helft G, Worthley SG, Beygui F, Zaman AG, Le Feuvre C, Vacheron A, Metzger JP, Badimon JJ, Fuster V. Identification of unstable coronary atherosclerotic plaques. *Arch Mal Coeur Vaiss*. 2001;94:583–590.
75. Wasserman BA, Smith WI, Trout HH III, Cannon RO III, Balaban RS, Arai AE. Carotid artery atherosclerosis: in vivo morphologic characterization with gadolinium-enhanced double-oblique MR imaging initial results. *Radiology*. 2002;223:566–573.
76. Kato S, Kitagawa K, Ishida N, Ishida M, Nagata M, Ichikawa Y, Katahira K, Matsumoto Y, Seo K, Ochiai R, Kobayashi Y, Sakuma H. Assessment of coronary artery disease using magnetic resonance coronary angiography: a national multicenter trial. *J Am Coll Cardiol*. 2010;56:983–991.
77. Lin R, Chen S, Liu G, Xue Y, Zhao X. Association between carotid atherosclerotic plaque calcification and intraplaque hemorrhage: a magnetic resonance imaging study. *Arterioscler Thromb Vasc Biol*. 2017;37:1228–1233.
78. Koktzoglou I. Gray blood magnetic resonance for carotid wall imaging and visualization of deep-seated and superficial vascular calcifications. *Magn Reson Med*. 2013;70:75–85.
79. Edelman RR, Flanagan O, Grodzki D, Giri S, Gupta N, Koktzoglou I. Projection MR imaging of peripheral arterial calcifications. *Magn Reson Med*. 2015;73:1939–1945.
80. Ferreira Botelho MP, Koktzoglou I, Collins JD, Giri S, Carr JC, Gupta N, Edelman RR. MR imaging of iliofemoral peripheral vascular calcifications using proton density-weighted, in-phase three-dimensional stack-of-stars gradient echo. *Magn Reson Med*. 2017;77:2146–2152.
81. Yoon YE, Hong YJ, Kim HK, Kim JA, Na JO, Yang DH, Kim YJ, Choi EY. 2014 Korean guidelines for appropriate utilization of cardiovascular magnetic resonance imaging: a joint report of the Korean Society of Cardiology and the Korean Society of Radiology. *Korean Circ J*. 2014;44:359–385.
82. Yuan C, Mitsumori LM, Beach KW, Maravilla KM. Carotid atherosclerotic plaque: noninvasive MR characterization and identification of vulnerable lesions. *Radiology*. 2001;221:285–299.
83. Saam T, Ferguson MS, Yarnykh VL, Takaya N, Xu D, Polissar NL, Hatsukami TS, Yuan C. Quantitative evaluation of carotid plaque composition by in vivo MRI. *Arterioscler Thromb Vasc Biol*. 2005;25:234–239.
84. Bornstedt A, Bernhardt P, Hombach V, Kamenz J, Spiess J, Subgang A, Rasche V. Local excitation black-blood imaging at 3T: application to the carotid artery wall. *Magn Reson Med*. 2008;59:1207–1211.
85. Chu B, Phan BA, Balu N, Yuan C, Brown BG, Zhao XQ. Reproducibility of carotid atherosclerotic lesion type characterization using high resolution multicontrast weighted cardiovascular magnetic resonance. *J Cardiovasc Magn Reson*. 2006;8:793–799.
86. Fabiano S, Mancino S, Stefanini M, Chiocchi M, Mauriello A, Spagnoli LG, Simonetti G. High-resolution multicontrast-weighted MR imaging from human carotid endarterectomy specimens to assess carotid plaque components. *Eur Radiol*. 2008;18:2912–2921.
87. Mujaj B, Lorza AM, van Engelen A, de Bruijne M, Franco OH, van der Lugt A, Vernooij MW, Bos D. Comparison of CT and CMR for detection and quantification of carotid artery calcification: the Rotterdam Study. *J Cardiovasc Magn Reson*. 2017;19:28.
88. Yang Q, Liu J, Barnes SR, Wu Z, Li K, Neelavalli J, Hu J, Haacke EM. Imaging the vessel wall in major peripheral arteries using susceptibility-weighted imaging. *J Magn Reson Imaging*. 2009;30:357–365.
89. Baheza RA, Welch EB, Gochberg DF, Sanders M, Harvey S, Gore JC, Yankeelov TE. Detection of microcalcifications by characteristic magnetic susceptibility effects using MR phase image cross-correlation analysis. *Med Phys*. 2015;42:1436–1452.
90. Fayad ZA, Fuster V, Nikolaou K, Becker C. Computed tomography and magnetic resonance imaging for noninvasive coronary angiography and plaque imaging: current and potential future concepts. *Circulation*. 2002;106:2026–2034.
91. Even-Sapir E, Metser U, Mishani E, Lievshitz G, Lerman H, Leibovitch I. The detection of bone metastases in patients with high-risk prostate cancer: 99mTc-MDP Planar bone scintigraphy, single- and multi-field-of-view SPECT, ^{18}F-fluoride PET, and 18F-fluoride PET/CT. *J Nucl Med*. 2006;47:287–297.
92. Blau M, Nagler W, Bender MA. Fluorine-18: a new isotope for bone scanning. *J Nucl Med*. 1962;3:332–334.
93. Hawkins RA, Choi Y, Huang SC, Hoh CK, Dahlbom M, Schiepers C, Satyamurthy N, Barrio JR, Phelps ME. Evaluation of the skeletal kinetics of fluorine-18-fluoride ion with PET. *J Nucl Med*. 1992;33:633–642.
94. Joshi FR, Rajani NK, Abt M, Woodward M, Bucerius J, Mani V, Tawakol A, Kallend D, Fayad ZA, Rudd JH. Does vascular calcification accelerate inflammation? A substudy of the dal-PLAQUE trial. *J Am Coll Cardiol*. 2016;67:69–78.
95. Buerger L, Oppenheimer A. Bone formation in sclerotic arteries. *J Exp Med*. 1908;10:354–367.
96. Jeziorska M, McCollum C, Wooley DE. Observations on bone formation and remodeling in advanced atherosclerotic lesions of human carotid arteries. *Virchows Arch*. 1998;433:559–565.
97. Cenizo Revuelta N, Gonzalez-Fajardo JA, Bratos MA, Alvarez-Gago T, Aguirre B, Vaquero C. Role of calcifying nanoparticle in the development of hyperplasia and vascular calcification in an animal model. *Eur J Vasc Endovasc Surg*. 2014;47:640–646.

98. Doherty TM, Fitzpatrick LA, Inoue D, Qiao JH, Fishbein MC, Detrano RC, Shah PK, Rajavashisth TB. Molecular, endocrine, and genetic mechanisms of arterial calcification. *Endocr Rev*. 2004;25:629–672.

99. Derlin T, Tóth Z, Papp L, Wisotzki C, Apostolova I, Habermann CR, Mester J, Klutmann S. Correlation of inflammation assessed by ^{18}F-FDG PET, active mineral deposition assessed by ^{18}F-fluoride PET, and vascular calcification in atherosclerotic plaque: a dual-tracer PET/CT study. *J Nucl Med*. 2011;52:1020–1027.

100. Derlin T, Wisotzki C, Richter U, Apostolova I, Bannas P, Weber C, Mester J, Klutmann S. In vivo imaging of mineral deposition in carotid plaque using 18F-sodium fluoride PET/CT: correlation with atherogenic risk factors. *J Nucl Med*. 2011;52:362–368.

101. Derlin T, Richter U, Bannas P, Begemann P, Buchert R, Mester J, Klutmann S. Feasibility of ^{18}F-sodium fluoride PET/CT for imaging of atherosclerotic plaque. *J Nucl Med*. 2010;51:862–865.

102. Beheshti M, Saboury B, Mehta NN, Torigian DA, Werner T, Mohler E, Wilensky R, Newberg AB, Basu S, Langsteger W, Alavi A. Detection and global quantification of cardiovascular molecular calcification by fluoro18-fluoride positron emission tomography/computed tomography—a novel concept. *Hell J Nucl Med*. 2011;14:114–120.

103. Basu S, Høilund-Carlsen PF, Alavi A. Assessing global cardiovascular molecular calcification with ^{18}F-fluoride PET/CT: will this become a clinical reality and a challenge to CT calcification scoring? *Eur J Nucl Med Mol Imaging*. 2012;39:660–664.

104. Morbelli S, Fiz F, Piccardo A, Picori L, Massollo M, Pestarino E, Marini C, Cabria M, Democrito A, Cittadini G, Villavecchia G, Bruzzi P, Alavi A, Sambuceti G. Divergent determinants of ^{18}F-NaF uptake and visible calcium deposition in large arteries: relationship with Framingham Risk Score. *Int J Cardiovasc Imaging*. 2014;30:439–447.

105. Fiz F, Morbelli S, Piccardo A, Bauckneht M, Ferrarazzo G, Pestarino E, Cabria M, Democrito A, Riondato M, Villavecchia G, Marini C, Sambuceti G. ^{18}F-NaF uptake by atherosclerotic plaque on PET/CT imaging: inverse correlation between calcification density and mineral metabolic activity. *J Nucl Med*. 2015;56:1019–1023.

106. Dweck MR, Jenkins WS, Vesey AT, Pringle MA, Chin CW, Malley TS, Cowie WJ, Tsampasian V, Richardson H, Fletcher A, Wallace WA, Pessotto R, van Beek EJ, Boon NA, Rudd JH, Newby DE. ^{18}F-sodium fluoride uptake is a marker of active calcification and disease progression in patients with aortic stenosis. *Circ Cardiovasc Imaging*. 2014;7:371–378.

107. Schinke T, Karsenty G. Vascular calcification: a passive process in need of inhibitors. *Nephrol Dial Transplant*. 2000;15:1272–1274.

108. Chen W, Dilsizian V. Targeted PET/CT imaging of vulnerable atherosclerotic plaques: microcalcification with sodium fluoride and inflammation with fluorodeoxyglucose. *Curr Cardiol Rep*. 2013;15:364.

109. Vesey AT, Jenkins WS, Irkle A, Moss A, Sng G, Forsythe RO, Clark T, Roberts G, Fletcher A, Lucatelli C, Rudd JH, Davenport AP, Mills NL, Al-Shahi Salman R, Dennis M, Whiteley WN, van Beek EJ, Dweck MR, Newby DE. (18)F-fluoride and (18)F-fluorodeoxyglucose positron emission tomography after transient ischemic attack or minor ischemic stroke: case-control study. *Circ Cardiovasc Imaging*. 2017;10:1–10.

110. Jenkins WS, Vesey AT, Shah AS, Pawade TA, Chin CW, White AC, Fletcher A, Cartlidge TR, Mitchell AJ, Pringle MA, Brown OS, Pessotto R, McKillop G, Van Beek EJ, Boon NA, Rudd JH, Newby DE, Dweck MR. Valvular (18)F-fluoride and (18)F-fluorodeoxyglucose uptake predict disease progression and clinical outcome in patients with aortic stenosis. *J Am Coll Cardiol*. 2015;66:1200–1201.

111. Fiz F, Morbelli S, Bauckneht M, Piccardo A, Ferrarazzo G, Nieri A, Artom N, Cabria M, Marini C, Canepa M, Sambuceti G. Correlation between thoracic aorta ^{18}F-natrium fluoride uptake and cardiovascular risk. *World J Radiol*. 2016;8:82–89.

112. Janssen T, Bannas P, Herrmann J, Veldhoen S, Busch JD, Treszl A, Münster S, Mester J, Derlin T. Association of linear ^{18}F-sodium fluoride accumulation in femoral arteries as a measure of diffuse calcification with cardiovascular risk factors: a PET/CT study. *J Nucl Cardiol*. 2013;20:569–577.

113. Li Y, Berenji GR, Shaba WF, Tafti B, Yevdayev E, Dadparvar S. Association of vascular fluoride uptake with vascular calcification and coronary artery disease. *Nucl Med Commun*. 2012;33:14–20.

114. George RT. ^{18}F-sodium fluoride positron emission tomography: an in vivo window into coronary atherosclerotic plaque biology. *J Am Coll Cardiol*. 2012;59:1549–1550.

115. Rosa GM, Bauckneht M, Masoero G, Mach F, Quercioli A, Seitun S, Balbi M, Brunelli C, Parodi A, Nencioni A, Vuilleumier N, Montecucco F. The vulnerable coronary plaque: update on imaging technologies. *Thromb Haemost*. 2013;110:706–722.

116. Blomberg BA, Thomassen A, Takx RA, Vilstrup MH, Hess S, Nielsen AL, Diederichsen AC, Mickley H, Alavi A, Høilund-Carlsen PF. Delayed sodium ^{18}F-fluoride PET/CT imaging does not improve quantification of vascular calcification metabolism: results from the CAMONA study. *J Nucl Cardiol*. 2014;21:293–304.

117. Slomka PJ, Pan T, Berman DS, Germano G. Advances in SPECT and PET hardware. *Prog Cardiovasc Dis*. 2015;57:566–578.

118. Bostrom K. Proinflammatory vascular calcification. *Circ Res*. 2005;96:1219–1220.

119. Li X, Heber D, Cal-Gonzalez J, Karanikas G, Mayerhoefer ME, Rasul S, Beitzke D, Zhang X, Agis H, Mitterhauser M, Wadsak W, Beyer T, Loewe C, Hacker M. Association between osteogenesis and inflammation during the progression of calcified plaque evaluated by 18F-fluoride and 18F-FDG. *J Nucl Med*. 2017;58:968–974.

120. Tawakol A, Migrino RQ, Bashian GG, Bedri S, Vermylen D, Cury RC, Yates D, LaMuraglia GM, Furie K, Houser S, Gewirtz H, Muller JE, Brady TJ, Fischman AJ. In vivo ^{18}F-fluorodeoxyglucose positron emission tomography imaging provides a noninvasive measure of carotid plaque inflammation in patients. *J Am Coll Cardiol*. 2006;48:1818–1824.

121. Figueroa AL, Abdelbaky A, Truong QA, Corsini E, MacNabb MH, Lavender ZR, Lawler MA, Grinspoon SK, Brady TJ, Nasir K, Hoffmann U, Tawakol A. Measurement of arterial activity on routine FDG PET/CT images improves prediction of risk of future CV events. *JACC Cardiovasc Imaging*. 2013;6:1250–1259.

122. Fayad ZA, Mani V, Woodward M, Kallend D, Abt M, Burgess T, Fuster V, Ballantyne CM, Stein EA, Tardif JC, Rudd JH, Farkouh ME, Tawakol A; dal-PLAQUE Investigators. Safety and efficacy of dalcetrapib on atherosclerotic disease using novel non-invasive multimodality imaging (dal-PLAQUE): a randomised clinical trial. *Lancet*. 2011;378:1547–1559.

123. Dalm VA, van Hagen PM, van Koetsveld PM, Achilefu S, Houtsmuller AB, Pols DH, van der Lely AJ, Lamberts SW, Hofland LJ. Expression of somatostatin, cortistatin, and somatostatin receptors in human monocytes, macrophages, and dendritic cells. *Am J Physiol Endocrinol Metab*. 2003;285:E344–E353.

124. Li X, Bauer W, Kreissl MC, Weirather J, Bauer E, Israel I, Richter D, Riehl G, Buck A, Samnick S. Specific somatostatin receptor II expression in arterial plaque: (68)Ga-DOTATATE autoradiographic, immunohistochemical and flow cytometric studies in apoE-deficient mice. *Atherosclerosis*. 2013;230:33–39.

125. Rominger A, Saam T, Vogl E, Ubleis C, la Fougère C, Förster S, Haug A, Cumming P, Reiser MF, Nikolaou K, Bartenstein P, Hacker M. In vivo imaging of macrophage activity in the coronary arteries using ^{68}Ga-DOTATATE PET/CT: correlation with coronary calcium burden and risk factors. *J Nucl Med*. 2010;51:193–197.

126. Li X, Samnick S, Lapa C, Israel I, Buck AK, Kreissl MC, Bauer W. ^{68}Ga-DOTATATE PET/CT for the detection of inflammation of large arteries: correlation with ^{18}F-FDG, calcium burden and risk factors. *EJNMMI Res*. 2012;2:52.

127. Tarkin JM, Joshi FR, Evans NR, Chowdhury MM, Figg NL, Shah AV, Starks LT, Martin-Garrido A, Manavaki R, Yu E, Kuc RE, Grassi L, Kreuzhuber R, Kostadima MA, Frontini M, Kirkpatrick PJ, Coughlin PA, Gopalan D, Fryer TD, Buscombe JR, Groves AM, Ouwehand WH, Bennett MR, Warburton EA, Davenport AP, Rudd JH. Detection of atherosclerotic inflammation by ^{68}Ga-DOTATATE PET compared to [^{18}F]FDG PET imaging. *J Am Coll Cardiol*. 2017;69:1774–1791.

128. Ryan TJ. The coronary angiogram and its seminal contributions to cardiovascular medicine over five decades. *Circulation*. 2002;106:752–756.

129. Picano E, Landini L, Distante A, Benassi A, Sarnelli R, L'Abbate A. Fibrosis, lipids, and calcium in human atherosclerotic plaque. In vitro differentiation from normal aortic walls by ultrasonic attenuation. *Circ Res*. 1985;56:556–562.

130. Picano E, Paterni M. Ultrasound tissue characterization of vulnerable atherosclerotic plaque. *Int J Mol Sci*. 2015;16:10121–10133.

131. Araki T, Banchhor SK, Londhe ND, Ikeda N, Radeva P, Shukla D, Saba L, Balestrieri A, Nicolaides A, Shafique S, Laird JR, Suri JS. Reliable and accurate calcium volume measurement in coronary artery using intravascular ultrasound videos. *J Med Syst*. 2016;40:51.

132. Nissen SE, Yock P. Intravascular ultrasound: novel pathophysiological insights and current clinical applications. *Circulation*. 2001;103:604–616.

133. Nair A, Margolis MP, Kuban BD, Vince DG. Automated coronary plaque characterisation with intravascular ultrasound backscatter: ex vivo validation. *EuroIntervention*. 2007;3:113–120.

134. Garcia-Garcia HM, Jang IK, Serruys PW, Kovacic JC, Narula J, Fayad ZA. Imaging plaques to predict and better manage patients with acute coronary events. *Circ Res*. 2014;114:1904–1917.

135. Kawasaki M, Bouma BE, Bressner J, Houser SL, Nadkarni SK, MacNeill BD, Jang IK, Fujiwara H, Tearney GJ. Diagnostic accuracy of optical coherence tomography and integrated backscatter intravascular ultrasound images for tissue characterization of human coronary plaques. *J Am Coll Cardiol*. 2006;48:81–88.

136. Mintz GS, Nissen SE, Anderson WD, Bailey SR, Erbel R, Fitzgerald PJ, Pinto FJ, Rosenfield K, Siegel RJ, Tuzcu EM, Yock PG. American College of Cardiology clinical expert consensus document on standards for acquisition, measurement and reporting of intravascular ultrasound studies (IVUS). A report of the American College of Cardiology Task Force on Clinical Expert Consensus Documents. *J Am Coll Cardiol*. 2001;37:1478–1492.

137. Okubo M, Kawasaki M, Ishihara Y, Takeyama U, Kubota T, Yamaki T, Ojio S, Nishigaki K, Takemura G, Saio M, Takami T, Minatoguchi S, Fujiwara H. Development of integrated backscatter intravascular ultrasound for tissue characterization of coronary plaques. *Ultrasound Med Biol*. 2008;34:655–663.

138. Tearney GJ, Yabushita H, Houser SL, Aretz HT, Jang IK, Schlendorf KH, Kauffman CR, Shishkov M, Halpern EF, Bouma BE. Quantification of macrophage content in atherosclerotic plaques by optical coherence tomography. *Circulation*. 2003;107:113–119.

139. Ijichi T, Nakazawa G, Torii S, Nakano M, Yoshikawa A, Morino Y, Ikari Y. Evaluation of coronary arterial calcification—ex-vivo assessment by optical frequency domain imaging. *Atherosclerosis*. 2015;243:242–247.

Key Words: atherosclerosis • calcification • imaging